Title
THE EFFECT OF SURFACE OXYGEN ON HYDROCARBON REACTIONS CATALYZED BY PLATINUM CRYSTAL SURFACES WITH VARIABLE KINK CONCENTRATIONS

Author
Davis, S.M.

Publication Date
1979-04-01

Lawrence Berkeley Laboratory
UNIVERSITY OF CALIFORNIA, BERKELEY, CA

Materials & Molecular
Research Division

Submitted to Surface Science

THE EFFECT OF SURFACE OXYGEN ON HYDROCARBON REACTIONS CATALYZED BY PLATINUM CRYSTAL SURFACES WITH VARIABLE KINK CONCENTRATIONS

S. M. Davis and G. A. Somorjai

April 1979

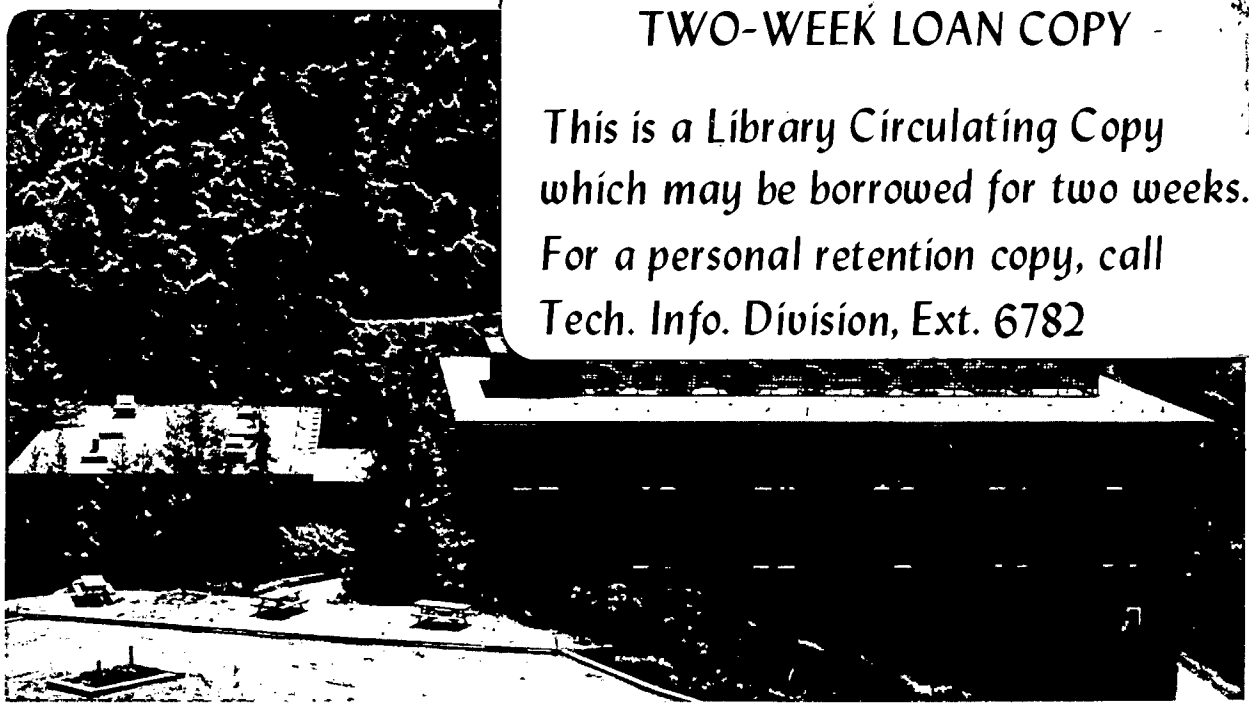

Prepared for the U. S. Department of Energy
under Contract W-7405-ENG-48

DISCLAIMER

LBL 8992

THE EFFECT OF SURFACE OXYGEN ON HYDROCARBON REACTIONS CATALYZED BY PLATINUM CRYSTAL SURFACES WITH VARIABLE KINK CONCENTRATIONS

S.M. Davis and G.A. Somorjai

Materials and Molecular research Division, Lawrence Berkeley Laboratory, and Department of Chemistry, University of California, Berkeley, CA 94720

April 1979

Prepared for the U.S. Department of Energy under Contract W-7405-ENG-48

Abstract

We have investigated the oxygen and hydrogen chemisorption properties and catalytic activities of the (12, 9, 8), (10, 8, 7), (654) and (321) platinum crystal surfaces which have (111) terraces, (410), (310) and (210) step orientations with 4.5, 5.9, 9.1 and 20% kink concentrations respectively. A UHV apparatus equipped for TDS, AES and LEED was utilized in these studies as a low pressure (10^{-5} - 10^{-6} torr) flow reactor. Partial oxidation of the terraces at 800°C in 10^{-7}-10^{-6} torr of O_2 enhanced the initial rates of cyclohexene hydrogenation and dehydrogenation and cyclohexane dehydrogenation. The ordered, ($\sqrt{3}x\sqrt{3}$)-R30°-O,oxygen layer was partially subsurface, strongly bound ($E_d \sim 60$ Kcal $mole^{-1}$ in zero coverage limit) and completely stable under reaction conditions in excess H_2. The enhancement in dehydrogenation activity at 150°C was greatest on the (10,8,7) platinum crystal surface with (310) step orientation (5.9% kinks). With a constant 5-atom terrace width the maximum activity shifted to higher oxygen coverage with increasing kink concentration. Strong chemisorption of hydrogen at kink sites was correlated with the greater resistance to self-poisoning of kinked surfaces as compared to Pt(111) and stepped Pt(557).

1. Introduction

The existence of strongly bound surface and subsurface oxygen is now well documented for most of the Group VIII transition metals, viz., Ni[1,2], Ru[3,4], Pd[5], Rh[6-10], Ir[11,12] and Pt[13-15]. The oxide-like surface compounds form irreversibly, usually at elevated temperatures, and have chemical properties distinctly different from oxygen chemisorbed at ambient or lower temperatures. The oxide layers are either ordered (Ni, Pd, Rh, Ir), epitaxially ordered (Ni, sometimes Pd and Pt), or disordered (Ru, Rh, Ir), depending upon the tendency for oxygen dissolution into the bulk and, thus, the near surface region oxygen:metal stoichiometry.

While all but a few studies have focused exclusively on characterization of the surface oxides, these compounds have marked influence on the catalytic behavior of transition metals. Virtually all commerical catalyst preparation procedures include calcination or other forms of oxygen pretreatment and temperatures where stable oxides form readily. An important question therefore concerns what effect strongly bound surface oxygen has on the catalytic activity, stability, and selectivity of Group VIII metals. Investigations of the effect of oxygen on the catalytic behavior of the flat Pt(111), stepped Pt(557) (or Pt(S)-[6(111)x(100)]), and kinked Pt(10,8,7) crystal faces have revealed[13] that the strongly bound oxygen on the high kink concentration surface imparts to it unique chemical activity: much enhanced dehydrogenation and hydrogenation rates during low pressure catalytic studies. Under the same conditions surface oxygen had little influence on the catalytic behavior of the flat (111) and

stepped platinum crystal surfaces. The combination of a surface kink site and strongly bound oxygen appears to be the decisive factor controlling the rate and selectivity of platinum in a variety of chemical reactions. Therefore, more detaled investigation of the chemical behavior of other kinked platinum surfaces in the presence of strongly bound oxygen are warranted.

We report here results of chemisorption (oxygen and hydrogen) and low pressure hydrocarbon catalysis studies for a series of platinum crystal surfaces with variable kink concentrations. It is shown that oxygen adsorbs at 800°C to form an ordered, near surface, oxide layer which activates the C-H bond breaking ability of kinked Pt crystal surfaces.

These kinked, oxygen pretreated platinum surfaces also exhibit resistance to self-poisoning, i.e. reaction inhibition by adsorbed hydrocarbons. Thermal desorption studies indicate that the increased strength of hydrogen binding at surface irregularities could be the cause of this effect.

2. Experimental

Experiments were performed in a stainless steel UHV apparatus equipped for thermal desorption (TDS), low energy electron diffraction (LEED) and Auger electron spectroscopy (AES). The base pressure was $\sim 8 \times 10^{-10}$ torr when the system was pumped by a 400 lit sec^{-1} Varion pump as in thermal desorption experments. Alternatively, an isolable 2" cryotrapped diffusion pump (base P $\sim 8 \times 10^{-9}$ torr)

enabled the system to operate as a low pressure flow reactor during crystal pretreatment and hydrocarbon catalysis studies. Conductance limited pumping speeds under these conditions were 11 lit sec^{-1} for H_2, 0.8 lit sec^{-1} for C_6H_{12}, and 0.5 lit sec^{-1} for C_6H_{10} and C_6H_6. Additional details of the apparatus were reported previously.[13]

Single crystals (ca. 1 mm thick and 1 cm^2) were spark eroded from a high purity Pt ingot (MRC) and polished according to standard procedures. Crystallographic orientations were determined by LEED and Laue back X-ray diffraction. The orientations studied and angles of cut relative to the (111) terrace plane and [01$\bar{1}$] zone axis are summarized in Table I. Idealized atomic surface structures expected for these orientations are illustrated in Fig.1. The (12, 9,8), (10, 8,7) and (654) surfaces have an almost constant 5-atom average terrace width and (410), (310) and (210) step orientations, respectively. The average separation between adjacent kinks thus varies from 4.8 to 10.0Å. The (321) crystal has (210) step orientation and 2-atom wide terraces.

The polished surfaces were cleaned <u>in situ</u> by argon ion sputtering at 800°C, annealing at 800-1100°C, and pretreatments with $\sim 2 \times 10^{-7}$ torr of O_2 at 1000°C. Five to ten 4-hour sputter-overnight anneal cycles were initially required to uniformly remove all traces of P, S, C, and Ca as detected by AES.

Oxygen was adsorbed by heating the crystals at 800°C in 5×10^{-8} - 5×10^{-6} torr of flowing O_2. The resulting surface oxygen did not react with H_2 below ~600°C and was completely stable under all reaction conditions. As described in detail elsewhere [13,16], approximate oxygen surface concentrations were calibrated from the O_{510}/Pt_{237}

Auger peak-to-peak height ratio. For Pt(654), Pt(10,8,7) and Pt(654), a ratio O_{510}/Pt_{237}=0.46-0.52 represented monolayer "coverage" based on discontinuities in plots of the adsorbate peak intensity against the substrate peak intensity. The average value of O_{510}/Pt_{237}=0.5=one oxygen monolayer was used below in the presentation of the catalytic results. Ease of oxidation followed the sequence Pt(12,9,8) $\gtrsim$ Pt(10, 8,7) $\sim$ Pt(654) $\gtrsim$ Pt(321).

To begin a reaction, hydrogen and hydrocarbon were introduced into the chamber at a total pressure of 10^{-4}-10^{-6} torr using variable leak valves. The catalyst samples were brought to reaction temperatures before admitting the hydrocarbon. The temperature was monitored continuously with a Pt-Pt/10% Rh thermocouple spot welded to the edge of the crystal, and all hydrocarbons (Matheson-"Spectroquality") were degassed by repeated freeze-pumping prior to use. Steady-state reaction rates were calculated using

$$TN_i = P_i S_i / RT_g N_s \qquad (1)$$

where TN_i was the turnover number for the formation of product i in molecules per surface Pt atom per second; P_i was the corrected partial pressure of species i; S_i was the pumping speed; T_g was 300 K; and N_s was the number of surface Pt atoms (ca. 1×10^{15}). Partial pressures were measured with the mass analyzer (UTI-100C) calibrated against a nude ion gauge for the gases of interest. Rates were corrected for background or system reactivity by running blank reactions with the crystal contaminated by an unreactive graphitic multilayer. The graphitic deposit formed after the crystals were heated in hydrocarbon at 650-800°C. Reproducibility in clean surface reactivity was better than $\pm$ 10% for C_6H_{10} dehydrogenation and

about ±15% for the other reactions.

3. Results

3.1 LEED Studies of the Oxidation of Kinked Pt Surfaces:

The clean surface LEED patterns for the crystals used in this investigation are illustrated in Fig.1. These orientations were stable in vacuum to over 1100°C.

Ordered oxygen structures were initially detected for Pt(654), Pt(10,8,7) and Pt(12,9,8) when the O_{510}/Pt_{237} Auger peak-to-peak height ratio was 0.20-0.25. As shown in Fig.2a for Pt(12,9,8) the predominant pattern was due to a $(\sqrt{3}x\sqrt{3})$-R30°-O structure on the (111) terraces. On Pt(10,8,7) the diffraction spots from the oxygen surface structure were occasionally split in the same direction as the diffraction spots due to the substrate, indicating that the oxygen layer was coherent over several terraces. On Pt(10,8,7) and Pt(12,9,8), with $0.25 \lesssim O_{510}/Pt_{237} \lesssim 0.4$, a less intense (2x2)-O structure sometimes coexisted with the $(\sqrt{3}x\sqrt{3})$-O structure. Only the $(\sqrt{3}x\sqrt{3})$-R30°-O structure was observed at $O_{510}/Pt_{237}=0.5$. The oxide "monolayer" has at least one oxygen atom for every three Pt surface atoms or about $5x10^{14}$ O atoms cm^{-2}. No ordered structures were detected for oxygen on Pt(321).

The growth of ordered multilayers was detected for Pt(12,9,8) and Pt(654) following extensive oxygen exposure at 800°C ($\gtrsim 10^3$ L). Oxide growth was accompanied by increased background intensity and gradual attenuation of the substrate diffraction features. The $(\sqrt{3}x\sqrt{3})$-R30°-O pattern observed for Pt(654) with

O_{510}/Pt_{237}=1.18 and 2-3% compressed ($\sqrt{3}x\sqrt{3}$)-R30° pattern (expanded structure) which emerged for Pt(12,9,8) with O_{510}/Pt_{237}=1.0-1.8 are shown in Figs. 2b and 2c, respectively. The latter pattern was also accompanied by weaker (1x4) diffraction features.

3.2 Thermal Desorption Studies of Chemisorbed Oxygen and Hydrogen:

The results of oxygen thermal desorption from Pt(12,9,8), Pt(10,8,7) and Pt(654) are shown in Fig.3. The crystals were exposed to O_2 at 800°C, cooled to ~50°C to obtain an Auger spectrum, and thereafter flashed to ~1150°C. The O_{510}/Pt_{237} ratio following a TDS run was $\lesssim$0.05 independent of the step orientation and initial oxygen coverage. The spectra for Pt(10,8,7) and Pt(654) were obtained with the crystal mounted on 0.5cm strands of 15 mil Pt wire. Heating rates were consequently non-linear and decreased from ~45Ksec^{-1} at 650°C to 15 Ksec^{-1} at 1050°C. For Pt(12,9,8) the crystal was specially mounted on Ta strips and carefully shielded by gold foils to expose only a crystal face in close line of sight to the mass spectrometer ionizer. In this configuration the heating rate was nearly constant at 25± 4K sec^{-1}.

At least two adsorption states (or site dependent manifolds thereof) apparently exist for strongly bound oxygen on each surface. The state with the lower desorption temperature (ca. 800°C) tended to populate first. The state with the higher desorption temperature (~950°C) began to populate before the first state reached saturation and, thereafter continued to grow on further O_2 exposure at 800°C. A similar desorption temperature (800-

900°C) was observed for subsurface oxygen on Pd(111) [5,17]. Both oxygen desorption peaks for Pt(12,9,8) had shapes and coverage dependences characteristic of 2nd order desorption kinetics. Desorption activation energies were estimated from deconvoluted spectra using Edward's expansion for 2nd order desorption kinetics[18]

$$E_D = 3.5255 \frac{RT_p^2}{\Delta W_{\frac{1}{2}}} \left[1-0.5673 \left(\frac{\Delta W_{\frac{1}{2}}}{Tp}\right) +0.2366 \left(\frac{\Delta W_{\frac{1}{2}}}{Tp}\right)^2 + \text{---}\right] \quad (2)$$

where $\Delta W_{\frac{1}{2}}$ was the desorption peak full width at half maximum and T_p was the temperature of the maximum desorption rate. For the first state E_D decreased from 62± 6 kcal mole^{-1} at low coverage to 46±6 kcal mole^{-1} near saturation. For the second state, E_D was constant at ∿63± 5 kcal mole^{-1}. These states apparently originate from oxygen atoms at and just below the topmost surface layer, albeit the precise positions remain uncertain. Dynamic AES experiments confirmed that oxygen atoms segregate at the topmost layer from the near surface region during cooling from 800°C, especially following extensive oxygen exposures.

Thermal desorption spectra for hydrogen chemisorbed at 35± 5°C on clean and oxygen pretreated Pt(12,9,8) and Pt(10,8,7) are shown in Fig.4. At least three distinct adsorption states were observed for each surface. The more tightly bound state (Tp≈220-230°C) exhibited 1st order desorption kinetics and populated first on each surface. This state had an initial sticking coefficient of at least 0.2 and a desorption activation energy of ∿30 Kcal mole^{-1}. It is centered 25K higher than any state previously reported for hydrogen on platinum (Pt(100) had a state with Tp ∿ 195°C[19]). We attribute this state to chemisorption at sites adjacent to kink atoms as it is

unique to and common among the kinked surfaces that were studied.

The state from which hydrogen desorbed at the lowest temperature (Tp ∿60-80°C) appeared at lower exposures than the intermediate state (Tp ∿ 140°C). As shown in Fig.5, the position of the intermediate state is virtually identical to that reported by Collins and Spicer[20] for H_2 chemisorption at monatomic (100) steps on Pt(557). A terrace state with 1st order desorption kinetics and Tp ∿60°C was also observed in their studies. Accordingly, we associate the Tp ∿60°C and Tp ∿140°C peaks with hydrogen chemisorbed at terraces and steps, respectively. As expected from the step to terrace atom concentration ratios the (Tp ∿140°C)/(Tp ∿225°C) peak area ratios at saturation were ∿ 3:1 and 2:1 for Pt(12,9,8) and Pt(10,8,7), respectively.

Apart from perhaps a minor increase in the initial sticking coefficients for the Tp ∿ 60°C and Tp∿140°C adsorption states, no appreciable differences existed between TDS results for the clean and oxygen pretreated surfaces. This result indicates that step sites were not blocked for hydrogen chemisorption by the strongly bound surface oxygen. In contrast, on Pt(110) [21] and Pt(111) [22], McCabe and Schmidt reported that surface oxygen created hydrogen binding sites with increased binding energy and Tp∿120-140°C.

3.2 Reaction Rate Studies on the Kinked Pt Surfaces:

a. Cyclohexene Dehydrogenation:

The dehydrogenation of cyclohexene to benzene was studied as a function of temperature on the clean surfaces and as a function of the O_{510}/Pt_{237} pph ratio at 150°C. Standard pressures utilized for these experiments were 6×10^{-8} torr C_6H_{10} and 1×10^{-6} torr H_2.

The temperature dependence of the dehydrogenation rate is shown in Fig.6. The turnover number, TN_m (benzene molecules formed per surface Pt atom per sec) consistently exhibited a maximum at about 120°C, and the apparent activation energy below the temperature of this maximum was small. The surfaces with 5-atom terraces behaved similarly, exhibiting the same small actuation energy of $Ea \sim 3$-4 Kcal $mole^{-1}$ for $T \lesssim 110$°C. The reaction required essentially no actuation energy on the (321) crystal plane.

The effect of surface preoxidation on cyclohexene dehydrogenation activity is shown in Fig.7. Oxidation enhanced the initial rate of the reaction on all four kinked platinum surfaces. The extent of enhancement depended on the terrace width and kink concentration. For a constant terrace width, the maximum enhancement in the rate of dehydrogenation varied from 60% to almost 3-fold and shifted to higher oxygen coverage with increasing kink concentration. As indicated in Fig.5, half "monolayer" ($\gtrsim 2.5 \times 10^{14}$ O atoms cm^{-2}) of strongly bound oxygen increased the dehydrogenation activity of Pt(654) at all temperatures.

As illustrated in Fig.8, TNm refers to the maximum in the time dependent reactivity, TN(t), that was observed 3-15 minutes after starting the reaction. This reaction, as well as the others we investigated, self-poisoned over a period of 0.5-10 hours, depending on the pressure, surface structure (Fig.8a), temperature (Fig.8b) and to some extent the oxygen coverage (Fig.8c). In all cases self-poisoning was accompanied by deposition of 60-90% of a monolayer of a disordered partially hydrogenated carbonaceous overlayer ($C_{237}/Pt_{237} \sim 3.2$ represents monolayer coverage).[16]

By flashing the crystals in vacuum and on stream to 150°C or higher temperatures following 100-200 minutes of reaction,

we determined that self-poisoning was slower and largely reversible

when the reaction temperature was below 120°C. Self-poisoning was irreversible and comparatively fast on all the surfaces above 140°C. At 150°C, a rapid initial decline in activity, complete within half an hour, was followed by a low level, steady state, benzene production rate which persisted for several hours before diminishing to the background level. As indicated in Fig.8a, kinked Pt(654) irreversibly poisoned slower than stepped Pt(557) which deactivated slower than low index Pt(111)[13] [Pt(654)<Pt(557)<Pt(111)]. The kinked surfaces deactivated at similar rates for a given reactant pressure, temperature and oxygen coverage. As shown in Fig.8c, surfaces oxidized to submonolayer coverages usually deactivated slower than clean surfaces, and both consistenly self-poisoned slower than platinum surfaces covered with oxide multilayers ($O_{510}/Pt_{237} \gtrsim 0.5$).

The hydrogen thermal desorption spectra in Fig.9 illustrate that after reactions at 150°C, the carbonaceous deposit contained about 10 times as much desorbable hydrogen as clean platinum surfaces saturated with H_2 at 35°C. After reactions at lower temperatures, the adlayer contained more benzene[23] and less desorbable hydrogen. At temperatures higher than 150°C benzene desorption was not detected and the hydrogen content was also reduced as compared to the amount of hydrogen that could be desorbed after reaction at 150°C.

b. Cyclohexene Hydrogenation.

Cyclohexene underwent hydrogenation as well as dehydrogenation under the conditions of our experiments. Turnover numbers for cyclohexane production as a function of oxygen coverage are shown

in Fig.10. Only the clean surfaces wtih (210) step orientation, viz. Pt(321) and Pt(654), exhibited measurable activity at 150°C. Hydrogenation required no activation energy ($E_a \lesssim 1$ kcal mole^{-1}) on these surfaces and accounted for less than 10% of the total cyclohexene conversion. The total conversion for the kinked surfaces was 0.3-3.5 product molecules per surface Pt atom in three hours. All the surfaces produced cyclohexane at measurable rates following oxygen pretreatment. Similar low-level hydrogenation activity was reported for stepped Pt(557) but not Pt(111) after preoxidation in an earlier study.[13]

The selectivity for hydrogenation ($TN_{\bigcirc}/TN_{\bigcirc}$) varied with the oxygen surface concentration and was maximized at coverages corresponding to the maxima in the hydrogenation activity; i.e. at O_{510}/Pt_{237}=0.0, 0.20, 0.12 and 0.25 for Pt(321), (654), (10,8,7) and (12,9,8) respectively. More importantly, hydrogenation selectivity correlated with the formation of the carbonaceous overlayer. The selectivity was 10-15% at the start of reaction but decreased rapidly during the first 15 minutes of reaction time. In situ AES analysis revealed that this time span is required to initially deposit roughly half a monolayer of hydrocarbon. Cyclohexene continued to dehydrogenate at a reduced rate in the presence of the overlayer after the hydrogenation reaction had self-poisoned.

c. Cyclohexane Dehydrogenation.

The dehydrogenation of cyclohexane to benzene was also investigated on the clean and oxidized surfaces. Results obtained at 150°C with 2×10^{-6} torr C_6H_{12} and 1×10^{-5} torr H_2 are illustrated in

Fig.10. The shapes of the curves were generally similar to those for cyclohexene dehydrogenation, but the reaction probabilities were about two orders of magnitude smaller. With a constant terrace width, the maximum activity shifted to higher oxygen coverages with increasing kink concentration. At $O_{510}/Pt_{237} \sim 0.2$, the Pt(10,8,7) crystal face exhibited a 3-fold activity enhancement over the clean platinum surface. Cyclohexene was sometimes produced as a minor dehydrogenation product ($TN_m \lesssim 2 \times 10^{-5}$ mole site^{-1} sec^{-1}) after two to four hours on stream. Results for a series of reactions with varying pressures are summarized in Table II. As indicated, the initial rate was approximately 1st order in hydrocarbon and fractional positive order in H_2 pressures. The parameter $t_{\frac{1}{2}}$ was the time required for the activity to drop to one-half its maximum value. It reflects that self-poisoning and adlayer buildup rates were inverse order in H_2 pressure and consistently slower than during cyclohexene dehydrogenation, even when the cyclohexane pressure was 25 times greater that.

4. Discussion

4.1 Reactivity of Oxygen Pretreated Platinum.

A $(\sqrt{3}x\sqrt{3})$-R30°-O structure was observed for the ordered oxygen layer independent of the substrate step orientation. Neither the $(\sqrt{3}x\sqrt{3})$-R30°-O structure for Pt(111) vicinal surfaces, nor the (2x2)-O structure for Pt(111) [13] seemingly correspond to epitaxial growth of PtO or PtO_2. Epitaxial growth of PtO was reported for Pt(110) at ~800°C.[14] The appearance of the bulk oxide coincidence mesh was preceeded in the coverage range spanning our studies by the formation

of a simpler c(2x2) transient oxide structure. Both ordered layers on Pt(110) decomposed at about 1000°C in reasonable agreement with our TDS results. Unique oxygen bonding states which exist in the near surface region stabilize the ordered layers at temperatures far exceeding the thermal decomposition of bulk oxides, e.g. 450-600°C for PtO_2 and PtO.[24]

It is possible for the kink sites along the step edges to be fully occupied by the oxygen atoms of a $(\sqrt{3}x\sqrt{3})$-R30°-0 overlayer structure when the step orientation is (210), (510), or (3n-1,10) with n an integer. Thermal desorption spectra for hydrogen chemisorbed along the (210), (310) and (410) step edges of Pt(654), Pt(10,8,7) and Pt(12,9,8) were not modified appreciably by oxygen pretreatment. These facts, along with a general absence of one dimensional ordering, suggest that the oxygen layer formed preferentially at or below the terraces and not in direct coincidence with the step edges.

The dehydrogenation activity of the kinked surfaces with 5-atom terraces was enhanced by low coverages of strongly bound surface oxygen. The maximum in activity shifted to higher oxygen coverage with increasing kink concentration. The maxima appeared at about the same coverage as the initial onset of ordering in the oxide layer and, also, at about the same coverage where the second oxygen adsorption state began to populate. The activity decreased sharply at higher coverages corresponding to a buildup of subsurface oxygen. The reactivity of all the surfaces dropped and attained the same low values at coverages we have associated with an oxide monolayer, i.e. $O_{510}/Pt_{237} \sim 0.5$.

The terrace width was also important in determining the catalytic activity. The reactivity of Pt(321) and its poisoning

behavior changed little with oxygen pretreatment. This is probably due to a steric effect since the Pt(321) terraces (ca. 5 Å) are barely wide enough to accommodate π-bonded cyclohexene or benzene molecules (Van der Waals radii 7.2-7.6 Å).

Significant oxygen induced activity enhancements were detected only for kinked platinum surfaces that also had wider terraces (5 atoms wide or ~14Å) of (111) orientation. A factor of two or more enhancement in reactivity was obtained by the combined presence of oxygen and kink sites on the surfaces. As noted earlier, surface oxygen was not notably effective in activating the C-H bond breaking activity of the low index (111) and stepped platinum surfaces. The resistance of the (111) and (557) platinum surfaces to self-poisoning was also unchanged by surface oxygen.[13] In contrast, on the kinked Pt(654), Pt(10,8,7) and Pt(12,9,8) crystal faces surface oxygen inhibited deactivitation, especially at lower temperatures and thus stabilized sites that would otherwise poison rapidly. Surface oxygen promoted both the activity and stability of the kinked surfaces with 5 atom wide terraces.

We have not observed any evidence for oxygen induced surface reconstruction, faceting, or compound formation between hydrogen and surface oxygen. The change in reactivity is apparently due to a change in the electronic structure of Pt atoms on kinked surfaces which result from charge transfer from platinum to oxygen.[13]

It should be emphasized that the hydrocarbon reactions we have investigated at low pressure are not strictly catalytic because the time integrated turnover frequencies were usually less than one product molecule per surface Pt atom. Nevertheless, there

are striking similarities between our results and results obtained near atmospheric conditions with supported catalysts. In studies of supported Pt by Poltorak and coworkers,[25] highly dispersed catalysts exhibited enhanced activity for cyclohexene hydrogenation after oxidation at 400°C. The activity of catalysts with low dispersions (i.e. crystallites $\gtrsim$ 50Å) was not altered appreciably. Mitrofanova, et al[26] reported similar behavior for cyclohexane dehydrogenation over supported Pt catalysts. These results are consistent with our own if we assume that highly dispersed particles have high concentrations of edge and kink sites while larger crystallites are more representative of (111) and stepped crystal faces. On the other hand, there are also significant differences between the results of high and low pressure studies since, at high pressures, these reactions often run without poisoning for many hours with a maximum reaction probability on the order of 10^{-7}.

4.2 Clean Surface Reactivity:

Among the clean surfaces at 150°C, Pt(321) (20% kinks) was distinctly more active for cyclohexane dehydrogenation and cyclohexene hydrogenation, but generally less active for cyclohexene dehydrogenation. The order of activities of the clean surfaces for cyclohexane dehydrogenation, (321)>(654)$\sim$(10,8,7)$\sim$(12,9,8)>(557)$\sim$(111), correlates to some extent with kink concentration. Nonetheless, the difference in reactivity between the least and most active planes was only about a factor of two. Our low pressure results concur with results for dispersed catalysts at high presssures[27,28] that indicate that cyclohexane dehydrogenation is essentially structure insensitive.

From the viewpoint of structure sensitivity, the most striking result of this study is that both clean surfaces with (210) step orientation [Pt(321) and Pt(654)] exhibited measurable hydrogenation activity at 150°C. Moreover, the hydrogenation activity was proportional to the density of monatomic (210) steps. The (12,9,8), (10,8,7),(557) and (111) crystal faces produced quantifiable amounts of cyclohexane only after the surfaces were preoxidized. It is interesting that Cunningham and Gwathmey [29] found a Ni(321) crystal to be at least a factor of two more active for ethylene hydrogenation than Ni(100), Ni(110) or Ni(111) in the first reactivity study using oriented crystal catalysts. Experimetns presently in progress should more decisively establish if sites associated with (210) steps are selectively active for olefin hydrogenation.

4.3 Poison Resistance of Kinked Pt Surfaces:

The cyclohexene dehydrogmation activity increased rapidly between 25 and 100°C. Thermal desorption studies[23] indicated that the benzene desorption rate becomes appreciable in this temperature range. The surfaces reversibly poisoned and saturated with benzene, or a precursor, when the reaction was carried out below the benzene desorption temperature of 120°C. At higher temperatures the rate decreased and the kinetics were dominated by rapid irreversible self-poisoning, At 150°C the deactivation rate was comparable to the benzene production rate.

Irreversible poisoning was facilitated by a rapidly decreasing concentration of chemi-

with increasing temperatures.
sorbed hydrogen. The residence time for the reacting species decreased more rapidly than the mean time necessary for benzene production as the steady state hydrogen coverage diminished with increasing reaction temperature. Hydrogen was chemisorbed tightly on the kinked surfaces and, consequently, kinked surfaces irreversibly poisoned more slowly than stepped Pt(557) or Pt(111). Comparison of Fig.5 with Fig.8 shows that the poisoning behavior and structure sensitivity of cyclohexene dehydrogenation correlate convincingly with the strength of the metal-hydrogen chemisorption bond. Surface hydrogen is an important additive inhibiting irreversible carbon buildup during low pressure hydrocarbon dehydrogenation.

5. Conclusions

Low concentrations of strongly bound surface oxygen enhance the C-H bond breaking of kinked Pt crystal surfaces and alter the product distribution during hydrocarbon hydrogenation and dehydrogenation. A combination of high surface kink concentration and the presence of strongly bound oxygen are needed to obtain this effect.

Chemisorbed hydrogen, bound strongly at surface kinks, also plays an important role in inhibiting irreversible self-poisoning reactions and concomitant buildup of carbonaceous deposits.

Similar phenomena, due to surface additives, are expected to be important for supported Pt catalysts where stable surface oxides could form during oxygen pretreatments or by chemical interactions between the metal particles and the oxide support. Hydrogen prevents self-poisoning of kinked Pt surfaces.

This work was supported by the Division of Materials Sciences, Office of Basic Energy Sciences, U.S. Department of Energy

References

1. P.R. Norton, R.L. Tapping and J.W. Goodale, Surface Sci. 65, 13 (1977).
2. P.H. Holloway and J.B. Hudson, Surface Sci. 43, 123 (1974).
3. R. Klein and A. Shih, Surface Sci. 69, 403 (1977).
4. P.D. Reed, C.M. Comrie and R.M. Lambert, Surface Sci. 64, 603 (1977).
5. H. Conrad, G. Ertl, J. Kuppers and E.E. Latta, Surface Sci.,65 245 (1977)
6. P.A. Thiel, J.T. Yates and W.H. Weinberg, Surface Sci. 82, 22 (1979).
7. D.G. Castner, B.A. Sexton and G.A. Somorjai, Surface Sci. 71 519 (1978).
8. C.W. Tucker Jr., J. Appl. Phys. 37, 4147 (1966).
9. C.W. Tucker Jr., J. Appl. Phys. 38, 2696 (1967).
10. D.G. Castner and G.A. Somorjai, Surface Sci. in press.
11. J.L. Taylor, D.E. Ibbetson and W.H. Weinberg, Surface Sci. 79, 349 (1979).
12. V.P. Ivanov, G.K. Boreskov, V.I. Savchenko, W.F. Egelhoff Jr. and W.H. Weinberg, Surface Sci. 61, 207 (1976).
13. C.E. Smith, J.P. Biberian and G.A. Somorjai, J. Catal. in press.
14. R. Ducros and R.P. Merrill, Surface Sci. 55, 227 (1976).
15. J.L. Gland and V.N, Korchak, Surface Sci. 75, 733 (1978).
16. J.P. Biberian and G.A. Somorjai, Appl. Surface Sci. 2, 253 (1979).
17. D.L. Weisman, M.L. Shek and W.E. Spicer, Surface Sci., in press.
18. D. Edwards, Surface Sci. 54, 1 (1976).
19. R.W. McCabe and L.D. Schmidt, Proc. 7th Intern. Vac. Cong. & 3rd Intern. Conf. Solid Surfaces, Vienna, 1201 (1977).

20. D.M. Collins and W.E. Spicer, Surface Sci. 69, 85 (1977).

21. R.W. McCabe and L.D. Schmidt, Surface Sci. 60, 85 (1976).

22. R.W. McCabe and L.D. Schmidt, Surface Sci. 65, 189 (1977).

23. S.M. Davis and G.A. Somorjai, Surface Sci., to be published.

24. J.C. Chaston, Platinum Metals Rev. 8, 50, (1964).

25. O.M. Poltorak and V.S. Boronin, Russ. J. Phys. Chem. 40, 1436 (1966).

26. A.M. Mitrafanova, V.S. Boronin and O.M. Poltorak, Russ. J. Phys. Chem. 46 32 (1972).

27. M. Boudart, A.W. Aldag, L.D. Ptak and J,E. Benson, J. Catal. 11, 35 (1968).

28. R.W. Maatman, P. Mahaffy, P. Hoekstra and C. Addink, J. Catal. 23, 105 (1971).

29. R.E. Cunningham and A.T. Gwathmey, Adv. Catal. 9, 25 (1957).

Figure Captions

Fig.1 Idealized atomic surface structures and LEED patterns for the platinum surfaces studied.

Fig.2 LEED patterns for ordered $(\sqrt{3}x\sqrt{3})$-R30° oxygen layers: (A) Pt(12,9,8), 45V O_{510}/Pt_{237}=0.38; (B) Pt(654), 105V, O_{510}/Pt_{237}=1.18; (C) Pt(12,9,8), 56V O_{510}/Pt_{237}=1.3.

Fig.3 Thermal desorption of O_2 from Pt(10,8,7), Pt(654) and Pt(12,9,8); 1 L = 10^{-6} torr sec.

Fig.4. Thermal desorption spectra for H_2 chemisorbed at 35±5°C on clean and oxygen pretreated Pt(10,8,7) and Pt(12,9,8).

Fig.5 Thermal desorption spectra for H_2 chemisorbed on flat Pt(111), stepped Pt(557) and kinked Pt(12,9,8). The lower curves are taken from Ref.20.

Fig.6 Temperature dependence of cyclohexene dehydrogenation to benzene with P_{HC}-$6x10^{-8}$ torr and P_{H_2}=1x10 torr.

Fig.7 Maximum turnover numbers at 150°C for the dehydrogenation of cyclohexene to benzene as a function of oxygen coverage.

Fig.8 Time dependent poisoning behavior during cyclohexene dehydrogenation to benzene at constant pressure ($6x10^{-8}$ torr C H and $1x10^{-6}$ torr H) (a) effect of surface structure; (b) effect of temperature; (c) effect of surface oxygen.

Fig.9 Comparison of hydrogen thermal desorption spectra for clean Pt(654) and Pt(654) following a three hour cyclohexene reaction at 150°C.

Fig.10 Maximum turnover numbers at 150°C for the hydrogenation of cyclohexene to cyclohexane as a function of oxygen coverage.

Fig.11 Maximum turnover numbers at 150°C for the dehydrogenation of cyclohexane to benzene as a function of oxygen coverage

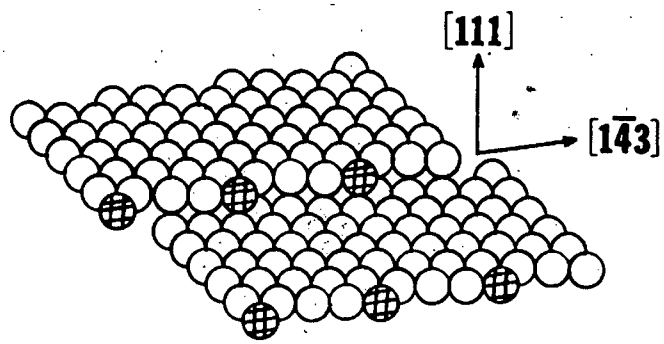

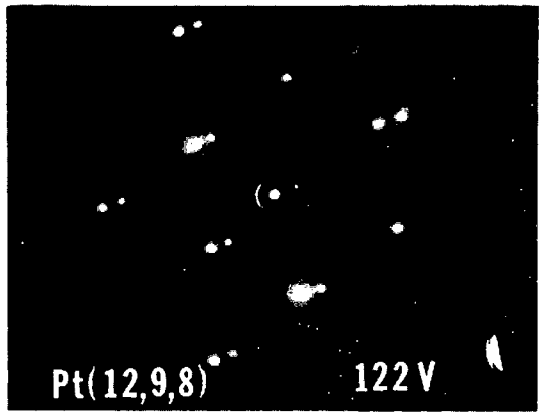

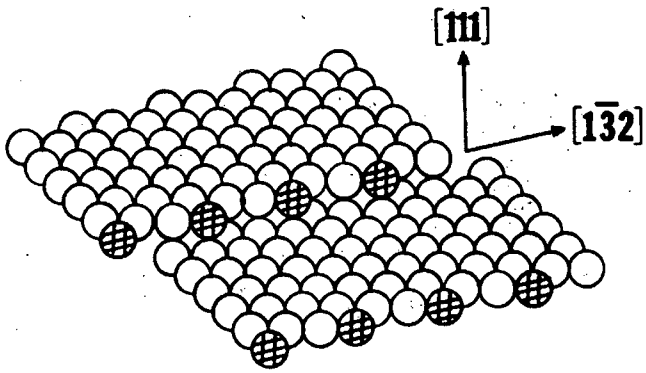

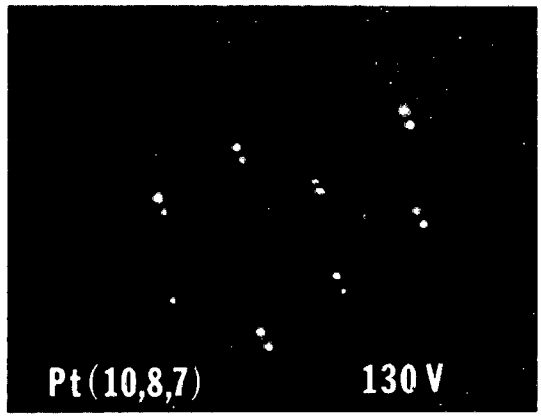

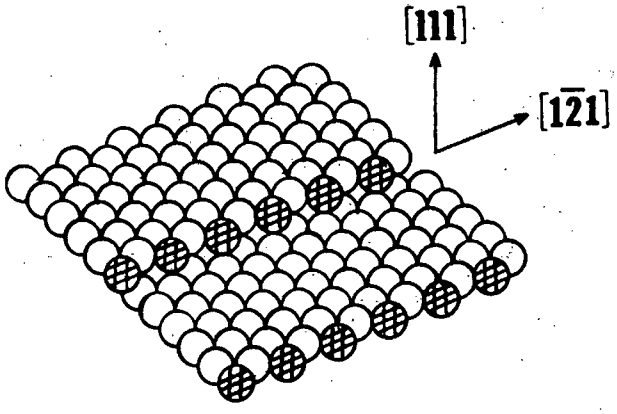

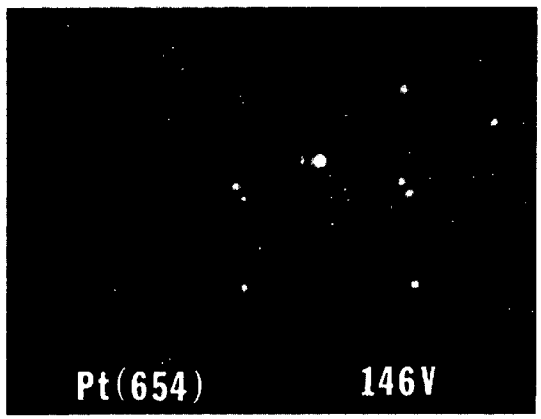

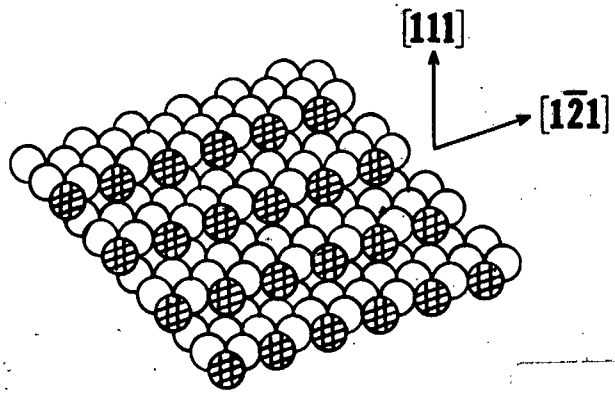

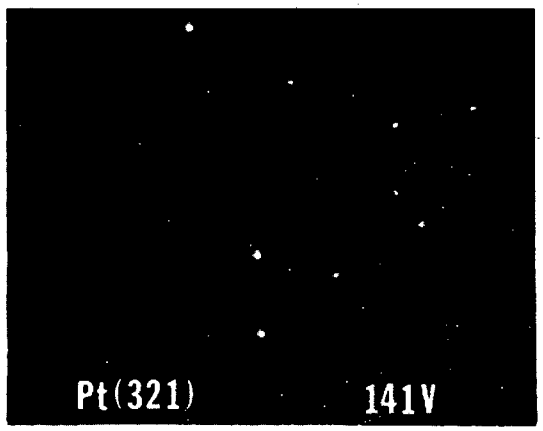

Fig.1

XBB 793-2960

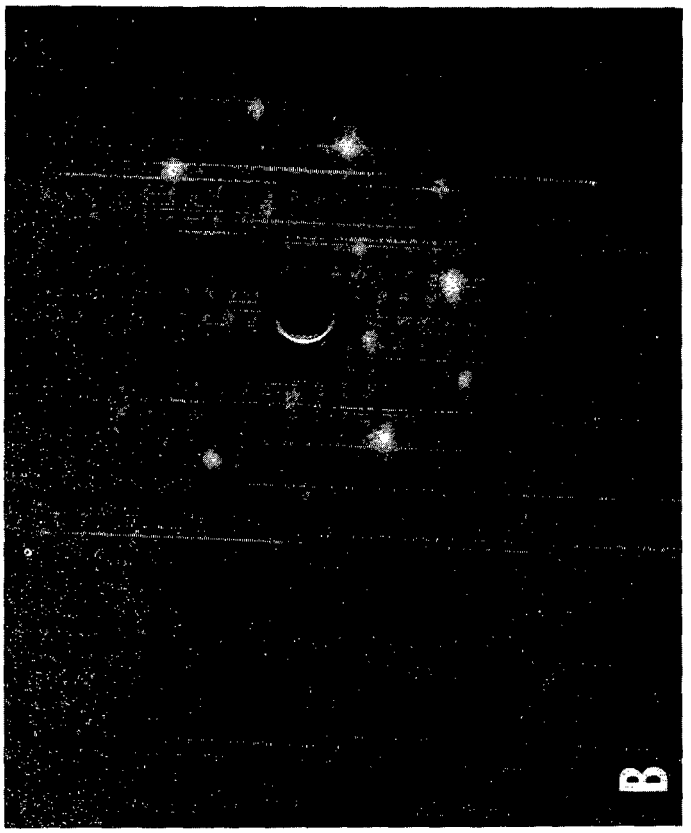

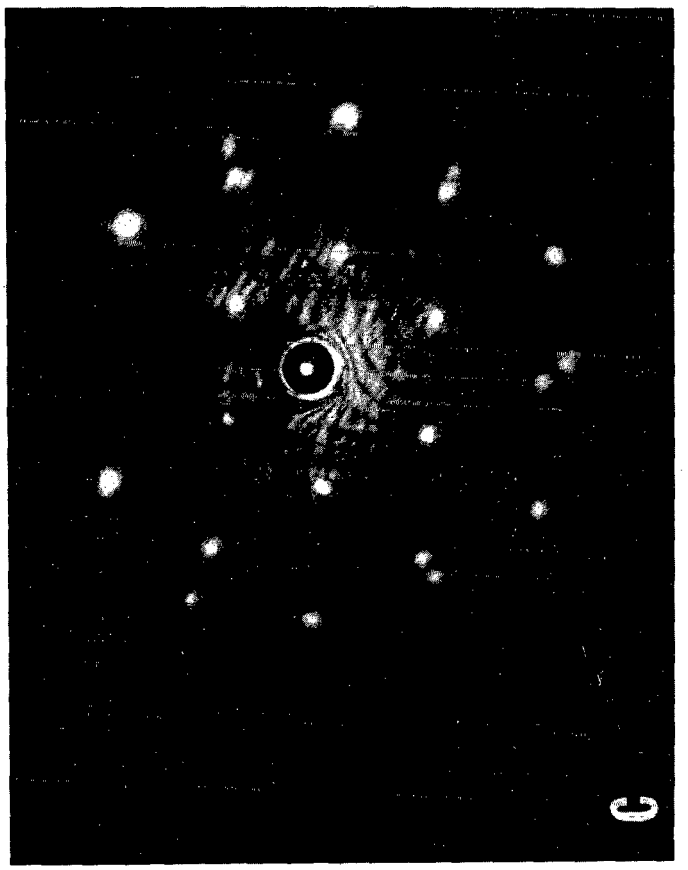

XBB 795-6638

Fig.2

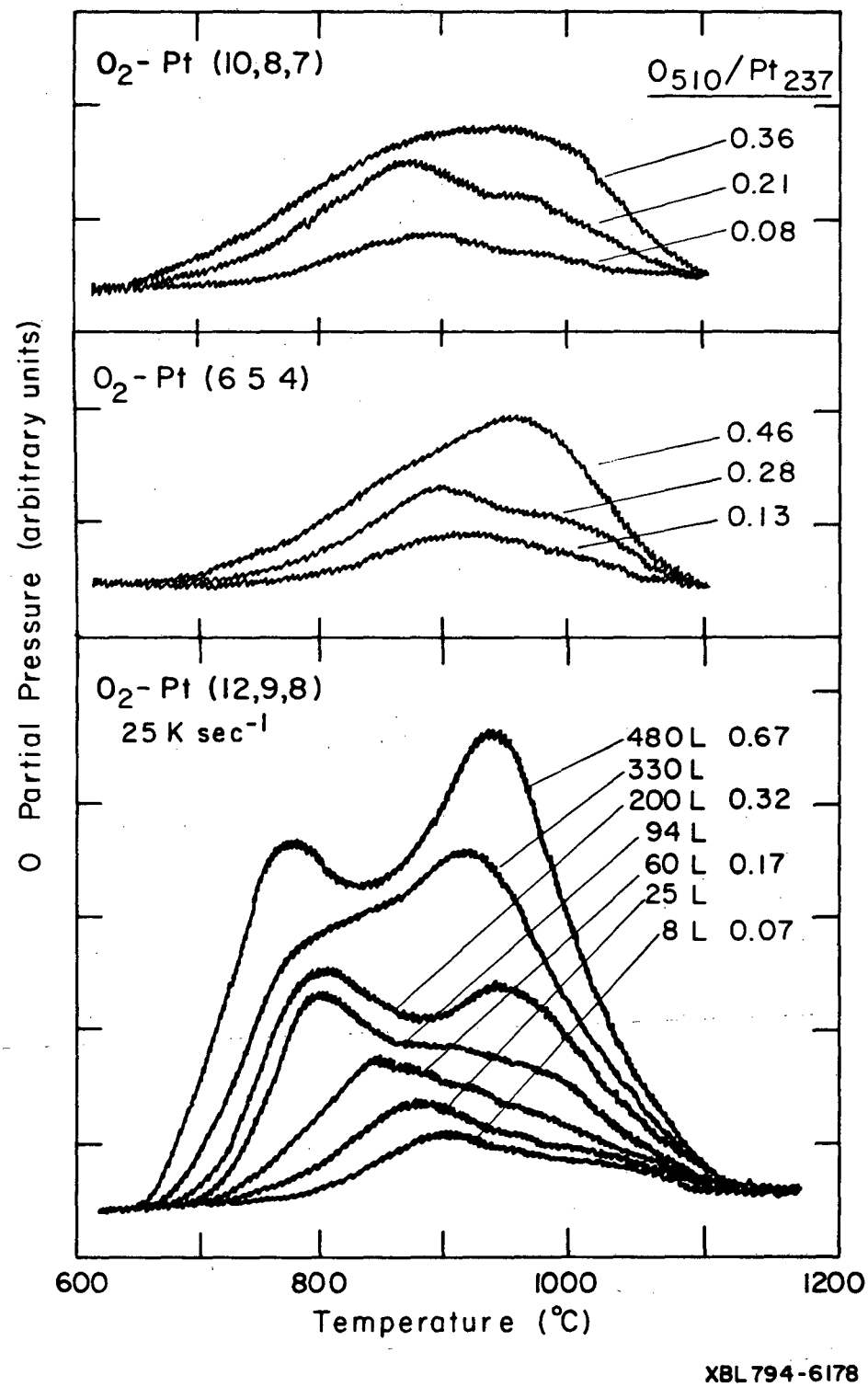
O_2- Pt (10,8,7)
O_{510}/Pt_{237}
0.36
0.21
0.08
O_2- Pt (6 5 4)
0.46
0.28
0.13
O_2- Pt (12,9,8)
25 K sec^{-1}
480 L 0.67
330 L
200 L 0.32
94 L
60 L 0.17
25 L
8 L 0.07
O Partial Pressure (arbitrary units)
600
800
1000
1200
Temperature (°C)
XBL 794-6178

Fig.3

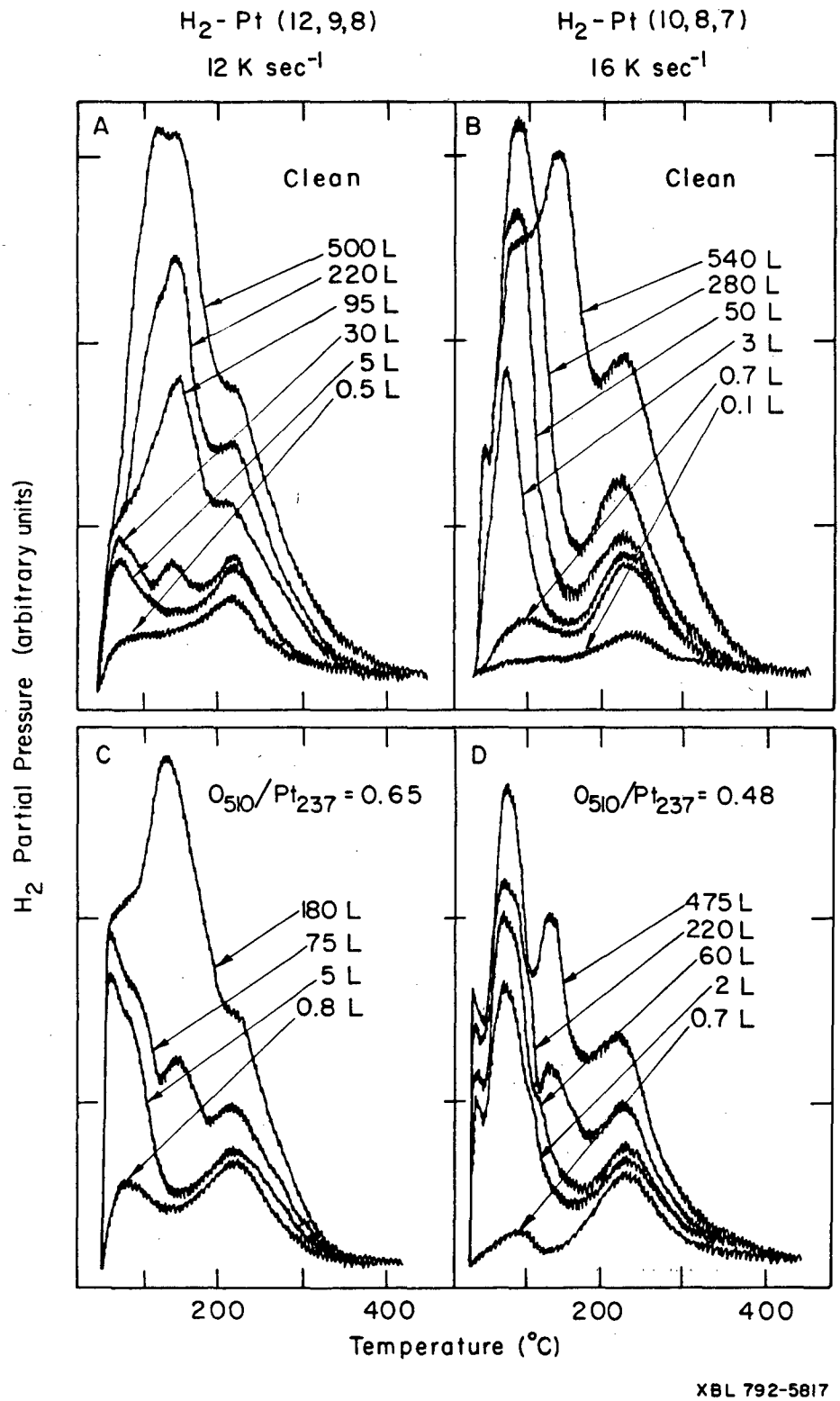
H2 - Pt (12, 9, 8)
12 K sec-1
H2 - Pt (10, 8, 7)
16 K sec-1
A
Clean
500 L
220 L
95 L
30 L
5 L
0.5 L
B
Clean
540 L
280 L
50 L
3 L
0.7 L
0.1 L
C
O510/Pt237 = 0.65
180 L
75 L
5 L
0.8 L
D
O510/Pt237 = 0.48
475 L
220 L
60 L
2 L
0.7 L
H2 Partial Pressure (arbitrary units)
200
400
200
400
Temperature (°C)
XBL 792-5817

Fig. 4

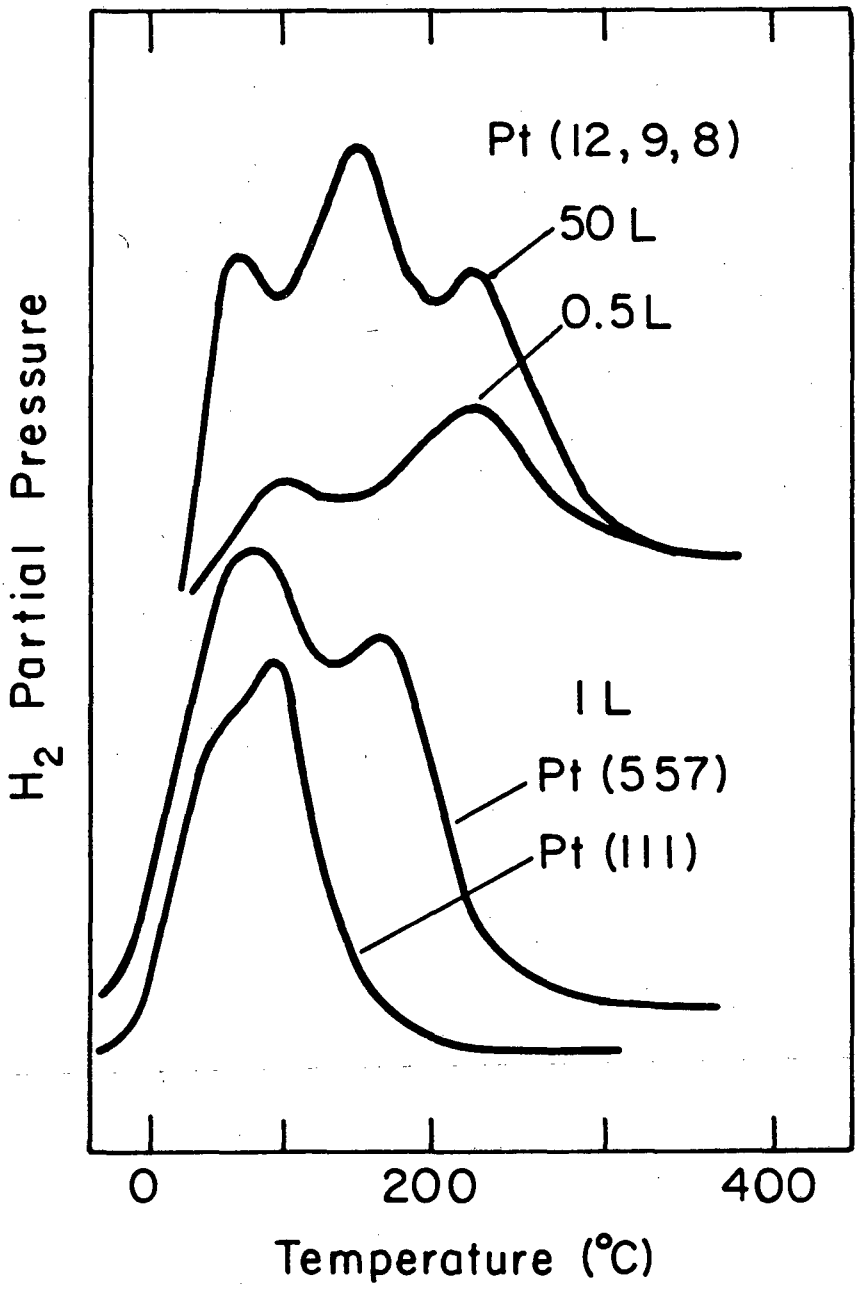

XBL 792-5816

Fig.5

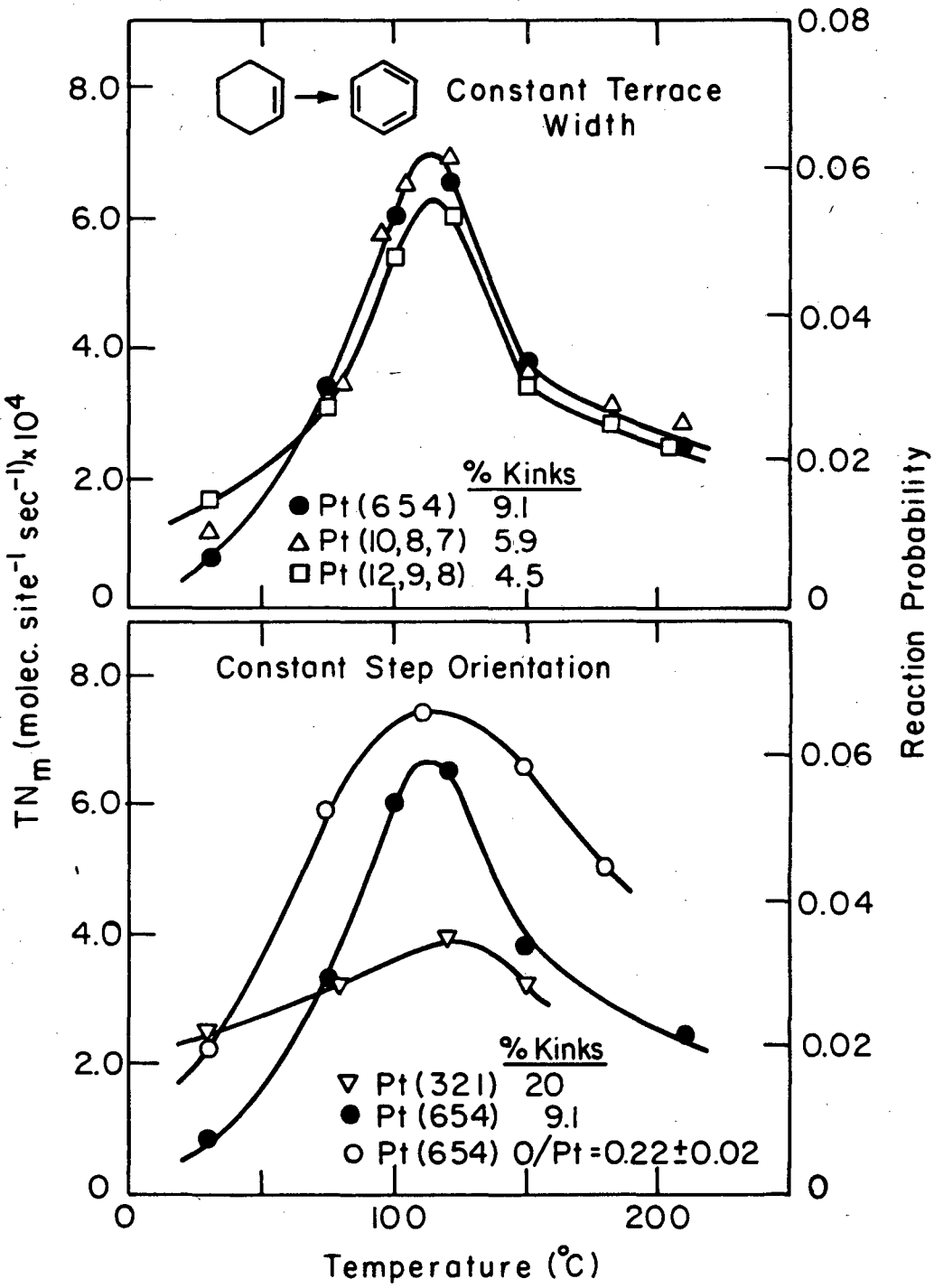

XBL792-5821

Fig.6

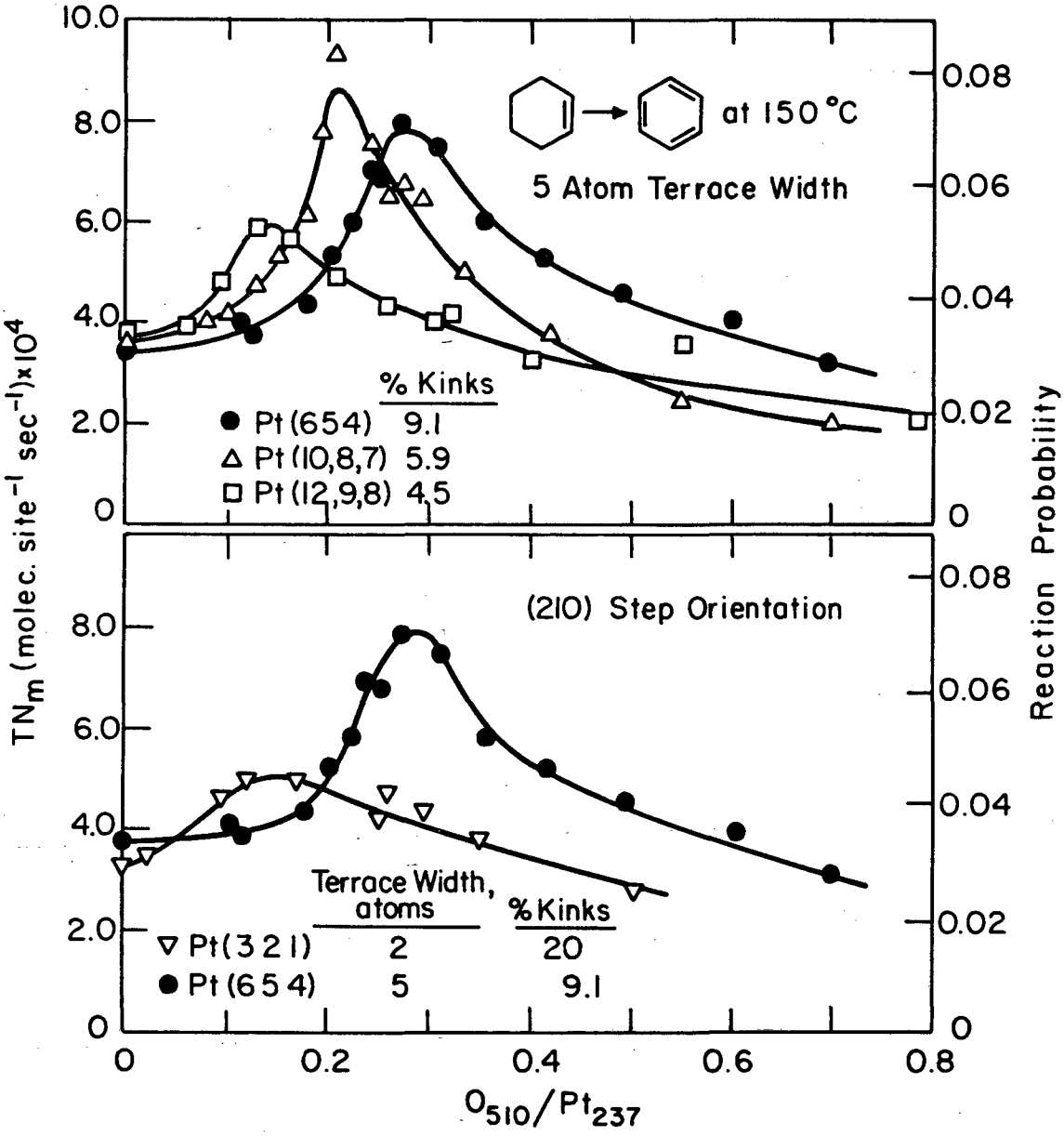
10.0
8.0
6.0
4.0
2.0
0
0.08
0.06
0.04
0.02
0
at 150 °C
5 Atom Terrace Width
% Kinks
Pt(654) 9.1
Pt(10,8,7) 5.9
Pt(12,9,8) 4.5
(210) Step Orientation
Terrace Width, atoms
% Kinks
Pt(321) 2 20
Pt(654) 5 9.1
0
0.2
0.4
0.6
0.8
O_{510}/Pt_{237}
TN_m (molec. site^{-1} sec^{-1})x10^4
Reaction Probability
XBL792-5824

Fig.7

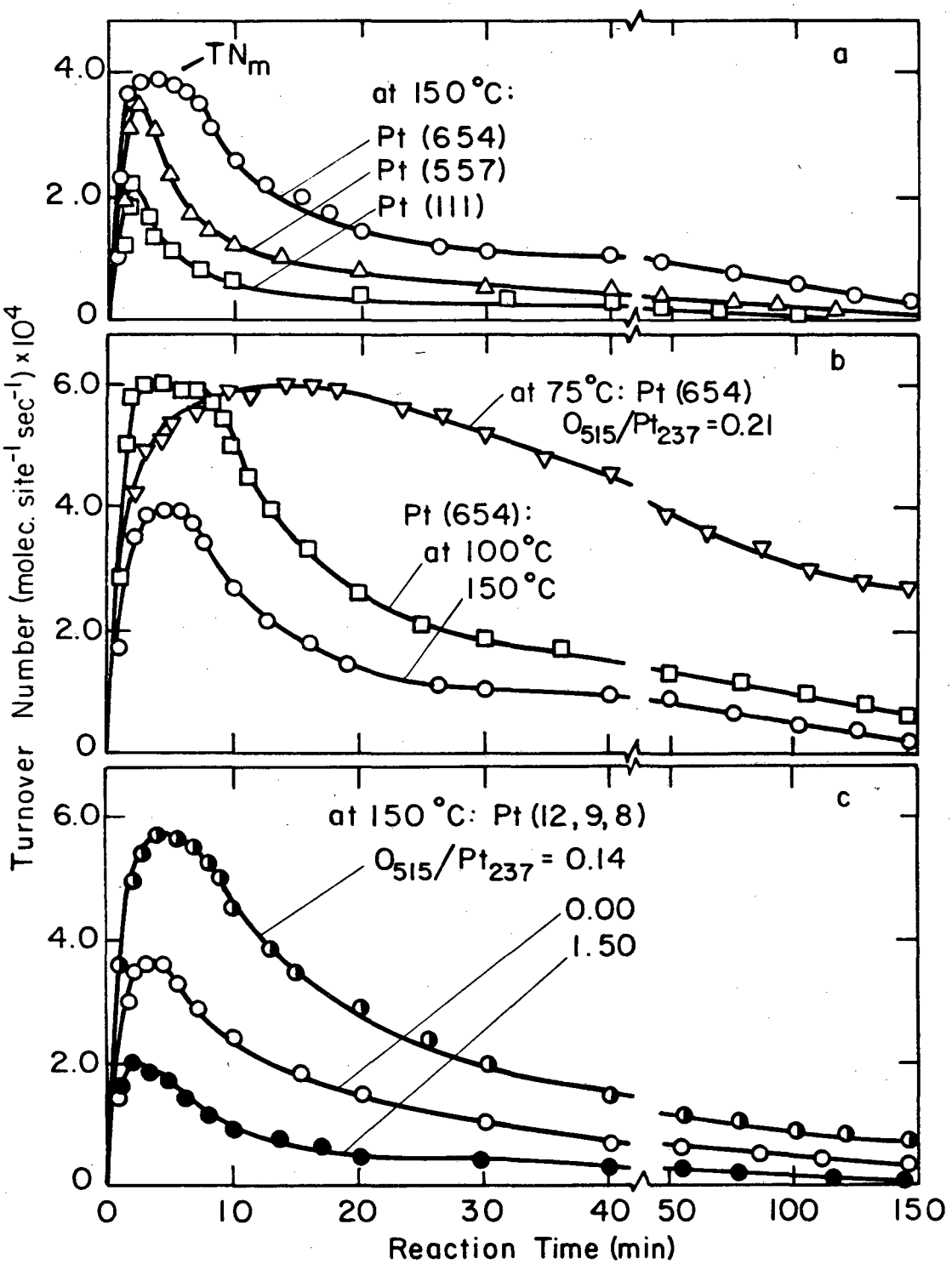
TNm
a
at 150 °C:
Pt (654)
Pt (557)
Pt (111)
b
at 75°C: Pt (654)
O515/Pt237 =0.21
Pt (654):
at 100°C
150 °C
c
at 150 °C: Pt (12, 9, 8)
O515/Pt237 = 0.14
0.00
1.50
Turnover Number (molec. site-1 sec-1) x10^4
Reaction Time (min)
0
10
20
30
40
50
100
150
2.0
4.0
6.0
XBL 794-6179

Fig.8

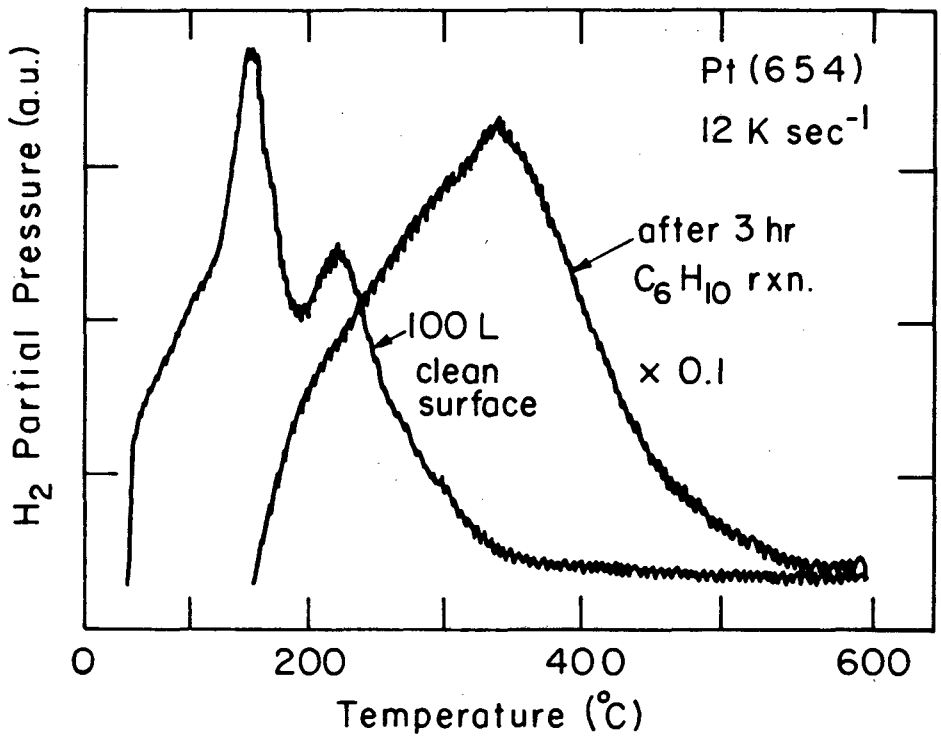

XBL792-5819

Fig.9

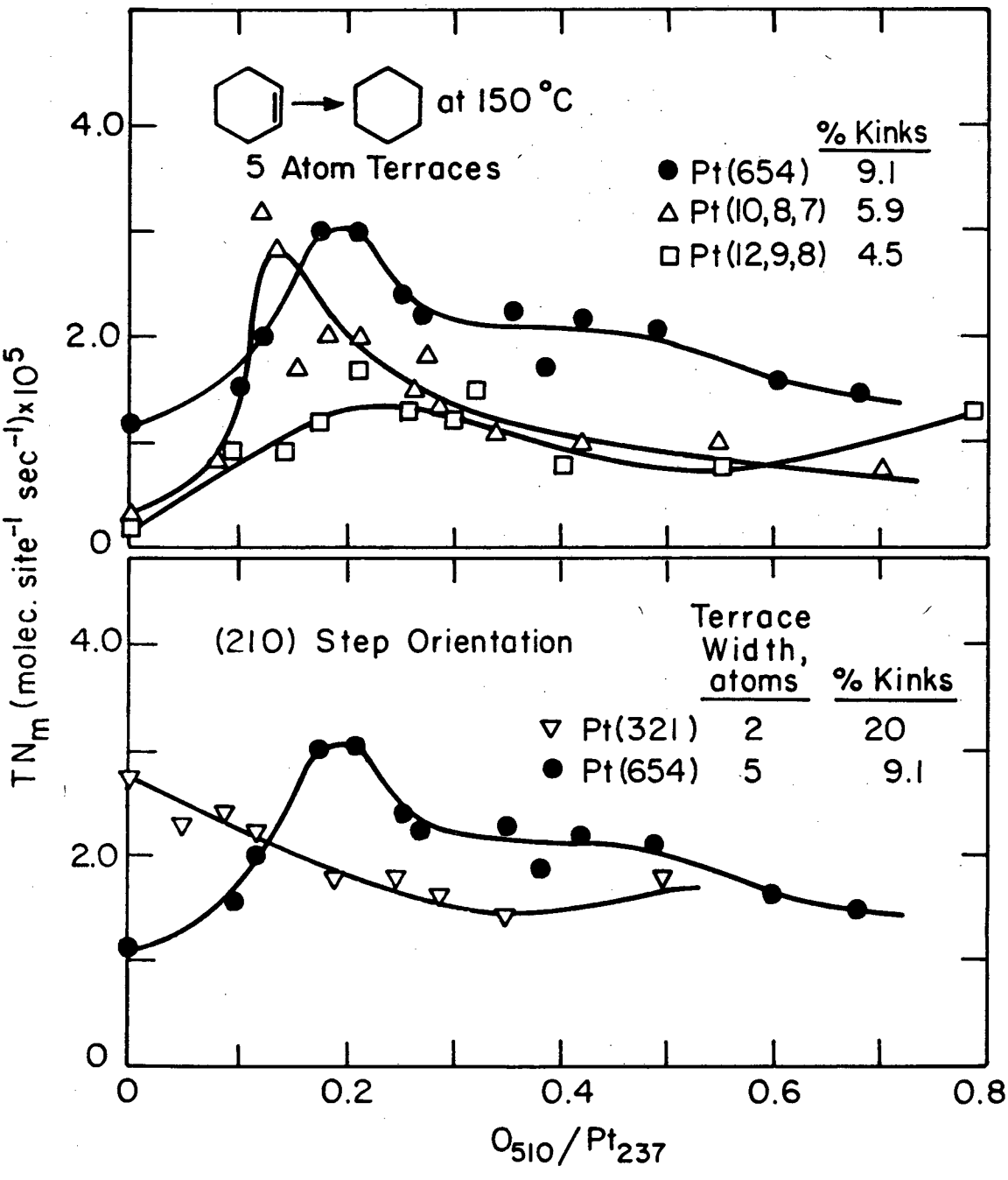

XBL792-5823

Fig.10

Fig.11

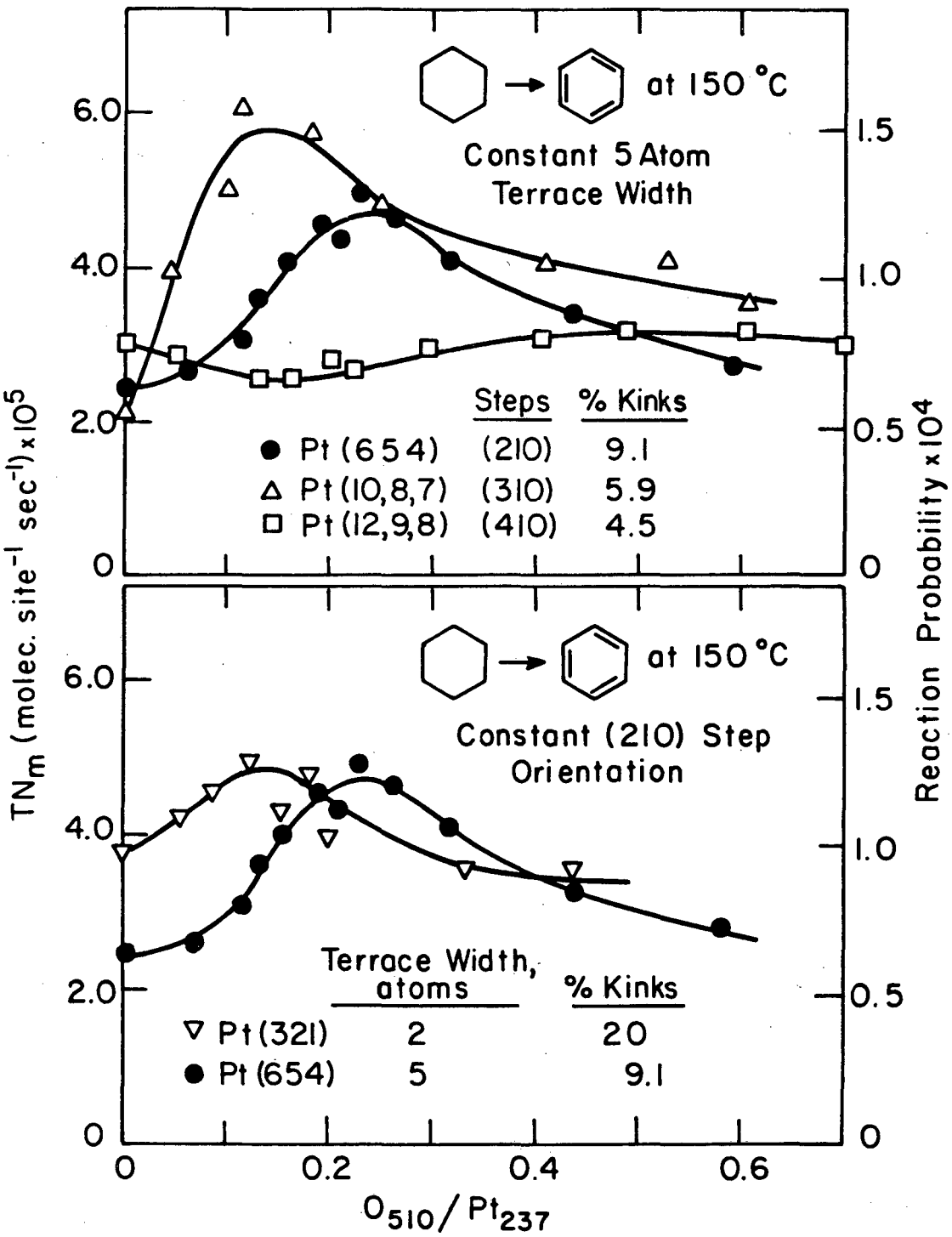

XBL792-5822

TECHNICAL INFORMATION DEPARTMENT
LAWRENCE BERKELEY LABORATORY
UNIVERSITY OF CALIFORNIA
BERKELEY, CALIFORNIA 94720